PCCP

Accepted Manuscript

ROYAL SOCIETY OF CHEMISTRY

www.rsc.org/pccp

Reversible Potentials for Steps in Methanol and Formic Acid Oxidation to CO_2; Adsorption Energies of Intermediates on the Ideal Electrocatalyst for Methanol Oxidation and CO_2 Reduction

by

Alfred B Anderson* and Haleema Asiri

Chemistry Department

Case Western Reserve University

Cleveland OH 44106-7078

*Corresponding Author

e-mail aba@po.cwru.edu

phone 216-368-5044

fax 216-368-3006

Abstract

Quantum chemical theory is used to identify the reasons for platinum's limitations as an electrocatalyst for oxidizing methanol at fuel cell anodes. The linear Gibbs energy relation (LGER) method is employed to predict reversible potentials for reaction steps for intermediates on the electrode surface. In this procedure standard reversible potentials are calculated for the reactions in bulk solution phase and then they are perturbed using calculated adsorption bond strengths to the electrode surface, yielding the equilibrium potentials for each electron transfer step for adsorbed intermediates. Adsorption properties of ideal electrocatalysts for the methanol oxidation are found by imposing the condition that the reversible potential of each electron transfer step equals that for the overall reaction. The adsorption bond strengths that provide the ideal properties also apply to formic acid oxidation and carbon dioxide reduction. It is instructive to think of the ideal electrocatalyst as a lens that focusses the reversible potentials for the n individual electron transfer steps to the reversible potential for the n-electron process. It is found that the ideal catalyst will adsorb many intermediates, including HOOC, CO, OCH, HOC, HOCH, $HOCH_2$, and OCH_3 more weakly than platinum, and OOCH and OH more strongly. For example, for one possible pathway it is necessary to weaken adsorption bond strengths for $HOCH_2$, HOCH, OCH, HOOC by about 0.5 eV, weaken adsorption CO by about 1.1 eV and strengthen OH adsorption by about 0.6 eV. These results imply a need for developing new multi-component catalysts.

A. Introduction

Reversible potentials for electron transfer steps involving intermediates bonded to elelctrocatalysts are important information for understanding electrocatalytic mechanisms. For methanol and formic acid electro-oxidation to CO_2 and for reduction of CO_2 to potential fuels and other products, they are unknown. Reversible potentials for the one-electron oxidation steps in bulk solution are, except for the water-hydroxyl radical equilibrium, also unknown. However, it is possible to calculate reversible potential for the bulk solution reactions accurately by using good quality quantum chemical determinations of reaction Gibbs energies. Results of such calculations are presented here. The calculated reversible potentials for the reactions in bulk solution, when perturbed by calculated adsorption bond strengths, yield predictions for reversible potentials for reaction intermediates bonded to the electrode surface. These predictions are used here as the basis, along with what is known about the electron-proton transfer activation energies, for an analysis of experimental observations in recent experimental literature for platinum electrodes. A goal of the work is to identify the steps that need improvement, that is, for which the focus on catalyst improvement should be made if these organic substances are to be efficiently used in fuel cells.

The six-electron electro-oxidation of methanol over known electrocatalysts, including platinum, is an inefficient process, operating at high overpotentials and with losses due to forming unwanted soluble two- and four-electron oxidation products. The adsorbed intermediate carbon monoxide is not oxidized to carbon dioxide unless the electrode potential is high enough to oxidize water molecules to adsorbed hydroxyl radicals. For platinum electrodes this puts the potential too close to the operating potential of the oxygen cathode, and this renders the voltage and power output for the fuel cell low. The standard reversible potential, U^0, for the six-electron

reduction to carbon dioxide is 0.032 V on the standard hydrogen electrode (SHE) scale. Unless specified differently, it may be assumed that the temperatures of the experimental work discussed below are close to standard ambient, 298 K.

Platinum is the electrode material that has been most studied for methanol electro-oxidation applications, but it is not a good six-electron catalyst. During 50 mVs^{-1} anodic potential sweeps from 0.05 V, the onset potential for electro-oxidation of 1.0 M methanol in 1.0 M $HClO_4$ (perchloric acid) is about 0.4 V on Pt(111) and Pt(110) electrodes; on Pt(100) electrodes there is a narrow peak between 0.3 V and 0.4 V followed by an onset to high current densities at about 0.6 V.[1,2] During anodic sweeps for Pt(111) and on polycrystalline Pt electrodes, CO_2 is observed to begin to form at around 0.4 V.[2] These are high overpotentials. Two oxidation products are seen in addition to CO_2, the desired six-electron oxidation product. They are HCOOH (formic acid) from four-electron oxidation, and H_2CO (formaldehyde) from two-electron oxidation.[1,2] In a methanol fuel cell, efficient six-electron reduction is the goal. An important fraction of the literature that is relevant to mechanisms was reviewed over a decade ago by Iwasita[2] and an extensive review paper was published recently by the Abruna lab.[3] The reader is referred to their papers for additional details.

During the six-electron oxidation of methanol at pH = 0.0, a water molecule is needed to supply an oxygen atom, two electrons, and two protons. The six-electron methanol oxidation reaction is

$$CH_3OH(aq) + H_2O(l) \rightarrow CO_2(g) + 6H^+(aq) + 6e^- \quad (1)$$

In acid electrolytes, water becomes oxidized to adsorbed OH radicals, OH(ads) on Pt(111) surfaces around 0.5 V-0.7V and to O(ads) around 0.8 V.[4-8] On higher index surfaces and on

defect sites, OH(ads) forms at lower potentials. Because CO_2 begins to form at 0.4 V on platinum, it is clear that at potentials less than 0.8 V, OH(ads) and not O(ads) is oxidant.

The platinum electrode is not entirely inert. In cyclic voltammograms taken in the absence of methanol, under-potential-deposited (upd) hydrogen atoms are responsible for observed current densities from > 0.05 V to ~ 0.4 V on Pt(111) and Pt(100) electrodes in acid electrolyte.[9,10] However, on the (100) electrodes OH(ads) is also deposited in the ~0.4 V - 0.7 V range of potentials,[9,10] and there is evidence for OH(ads) deposition above 0.2 V on Pt(110) electrodes.[9] Thus OH(ads) is available at very low potentials on polycrystalline platinum electrodes since they provide a combination of adsorption sites and this accounts for CO(ads) oxidation at around 0.4 V.

Blocking of methanol adsorption by upd hydrogen may affect the overpotential for methanol oxidation, allowing oxidation only when the upd H(ads) coverage is low enough. Strmcnik et al. found that at 0.05 V, where H evolution commences during cathodic sweeps from the double layer region, the upd H(ads) coverage on Pt(111) was only about 0.67 ML.[10] Using quantum theory, a coverage of 0.72 ML, at 0.05 V, which supports the measurement, has been calculated.[11] Strmcnik et al. extrapolated to a maximum coverage of 0.88 ML at -0.1 V[10] and our predicted maximum coverage was 0.91 ML, also at -0.1 V.[11] The upd H(ads) dependence on potential was nearly linear between 0.05 V and 0.4 V, showing Frumkin behavior, and curvature at the ends apparently dominated by the Langmuir isotherm.[10,11] This means upd H(ads) will block Pt(111) electrode surface sites against adsorbing methanol and water at 0.05 V, which is the observed onset for H_2 evolution, and at slightly higher potentials. The coverage of upd H(ads) decreases as the potential is increased from 0.05 V, and measurement and theory showed the coverage drops to ½ ML at about 0.12 V.[10,11] It is likely that when upd H(ads) coverage

becomes less than ½ ML there will be adjacent Pt sites available to adsorb the intermediates that must form prior to forming H_2CO, HCOOH, CO(ads), or CO_2. In fact, CO(ads) has been seen by infrared spectroscopy to begin to form at about 0.2 V on a Pt(111) electrode in 1.0 M CH_3OH in 0.1 M $HClO_4$.[1,2] A strong CO(ads) signal forms on a Pt(110) electrode even at 0.1 V,[1,2] which is consistent with the narrow upd H(ads) potential range on this electrode.[9] It has been found that methanol oxidation is suppressed when CO(ads) coverage is greater than 0.33 ML.[3,12]

From the above, it is reasonably concluded that electro-oxidation of methanol proceeds over platinum(111) electrodes in acid electrolyte when the potential increases from the H_2 evolution potential of about 0.05 V to around 0.2 V, a potential with small enough coverage of upd H(ads). Some level of coverage by CO(ads) is achieved and when a potential of about 0.4 V is reached, its oxidation to CO_2 commences.[2] This oxidation requires the formation of OH(ads) from oxidation of water molecules,

$$H_2O(ads) \rightarrow OH(ads) + H^+ + e^- \qquad (2)$$

Evidently, the oxidation steps up to CO(ads) formation do not contribute to the overpotential. The overpotential evidently corresponds to the reversible potential for the reaction in eq (2). This would mean that the reversible potentials for the four one-electron transfer oxidation steps leading up to forming CO(ads) are no greater than 0.2 V. One of the goals of this study was to find out if this is true by means of theoretical calculations of the reversible potentials.

Activation energies for reactions of the surface intermediates occurring by the electron and proton transfers and for chemical reactions with no electron transfer are important for characterizing and understanding the mechanisms and rates for forming intermediates and CO_2. They will be functions of the electrode potential and therefore may decrease oxidation current

densities when the electrode potential is decreased and increase them when the potential is increased.

Finding activation energies experimentally requires measurements at several temperatures for each potential so that an Arrhenius slope can be generated for each potential. The Abruna group recently made a number determinations of effective activation energies for the electro-oxidation of methanol on a polycrystalline Pt electrode.[3] A significant dependence on the state of the electrode was identified. The electrode was either held at 1.2 V (Ag/AgCl) and then swept at 10 mVs^{-1} in the cathodic direction to -0.22 V (Ag/AgCl) or held at -0.22 V (Ag/AgCl) and swept at 10 mVs^{-1} in the anodic direction to 1.2 V (Ag/AgCl). The methanol concentrations were 0.5 M in three different electrolytes: 0.1 M H_2SO_4, 0.1 M $HClO_4$, and 0.1 M KOH. Current densities for generating the Arrhenius slopes were chosen for the desired potentials during the sweeps. Differences between effective activation energies at the same potential that were found during the anodic and cathodic sweeps were related to the excess O(ads) and OH(ads) formed at the high potential at the start of the cathodic sweeps. During cathodic, sweeps the activation energy, 0.7 eV at about 0.8 V(SHE) decreased rapidly to 0.33 eV at about 0.69 V, and then decreased slowly to 0.25 eV at about 0.62 V . The effective activation energy 0.25 eV is low.

B. Theoretical approach

Activation energies for many coupled electron-proton transfer reactions have already been calculated using quantum theory and a local reaction center model wherein electron transfer is assumed to take place by non-radiative tunneling from the electrode region surrounding the reaction center to the reaction center. Reduction occurs when the structure of the reaction center has an electron affinity, EA, equal to the electrode potential U(SHE) plus φ, the thermodynamic

work function of the standard hydrogen electrode.[13] This concept can be traced to the 1930's model of Gurney.[14] For oxidation the ionization potential, IP, is the adjustable variable.

In implementation, the hydronium ions or hydroxyl ions participating in the electron transfer are coordinated by water molecules and are either in the bulk solution or taken to be adsorbed on a small cluster of Pt atoms. A Madelung potential is added that represents the electrolyte charge distribution and the electrode is assigned a Fermi level corresponding to the electrode potential of interest.[15] At resonance during oxidation, an electron tunnels from the reaction center to empty band orbitals at the Fermi level, and during reduction, an electron tunnels from filled band orbitals at the Fermi level to the reduction center. There are multiple structure parameters to vary in the local reaction center model and many structures will be in resonance with the electrode Fermi level. The most stable of these structures is found using constrained variation theory, and this is the transition state structure. The energy to reach it, beginning from the hydrogen-bonded precursor complex, is the activation energy. Reactions already studied this way included upd H(ads) formation, H_2 oxidation, hydrogen evolution on diamond, and the steps in O_2 reduction to water, all in acid and some in base. References may be found in a review of the method.[16]

In every previous study using the local reaction center theory, the activation energy at the calculated reversible potential, which is the crossing point of the oxidation and reduction activation energy curves, was small. For example, it was less than 0.1 eV for the reaction in eq (2), water oxidation and OH reduction on platinum.[16] As mentioned above, experimentally determined effective activation energies were also low, 0.25 eV.[3] The shapes of the activation energy curves as functions of potential were such that at a few tenths of an eV positive of the calculated reversible potential for the adsorbed reactant and product, $U_{\mathrm{surf}}^{\mathrm{rev}}$, the activation energy for the oxidation reaction drops to zero and at a few tenths of an eV negative of $U_{\mathrm{surf}}^{\mathrm{rev}}$ the

activation energy for the reduction reaction drops to zero. This is depicted schematically in Figure 1. Thus, the selection criterion for easy or fast vs. difficult or slow reaction at the reversible potential for the overall many-electron process is based on whether the reversible potential for the step less than or more than the reversible potential for the full many-electron reaction. Comparable behavior is assumed for the reactions studied here, though an exception is suggested for oxidation of the adsorbed formyloxy radical, OCHO(ads), as will be discussed later.

The approach to calculating reversible potentials for each of the one-electron transfer steps during methanol oxidation to CO_2 is called the linear Gibbs energy relationship, LGER. To use this theory, the standard reversible potentials, U^0, for reactions of the intermediates solvated in bulk solutions must be known. The reactant and product molecules are perturbed by adsorption to the electrode surface and the adsorption energies of the intermediates are used to calculate the reversible potentials for the surface reactions from the bulk solution values. Standard reversible potentials for the surface reaction, U^{rev}_{surf}, are thereby predicted. When adsorption Gibbs energies are used, the procedure gives predictions within about 0.2 V of the most accurate values.[17] When adsorption internal energies are used in their place, the procedure is the approximate LGER theory, and this is the approach used in this paper. Its accuracy is close to that when Gibbs adsorption energies are used. This procedure has been reviewed recently.[17] The formalism is presented below.

Only one of the reversible potentials for the reactions of intermediates in bulk solution is known, 2.72 V for eq (2).[18] It was therefore necessary to calculate all of the others, which was done using density functional theory, including solvation and electrolyte ion distribution in a modified Poisson Boltzmann approach.[19,20] The code, called Interface, uses an atomic orbital

basis which makes calculations of one- and two-dimensional systems possible and allows the electrode potentials for them to be found as a simple function of the Fermi energy. The electrolyte concentration was 1.0 M and 3.0 Å radii were used for the ions. The temperature was 298.15 K. The theory is described in its entirety in Ref. 20. Altogether, 17 intermediate reactions were considered in the solution phase, and U^0 was calculated for one-electron plus proton transfers within pairs of them.

The formalism for determining the U^0 is as follows. For the reaction,

$$\mathrm{Ox(aq)} + \mathrm{e^-}(U^o) \rightleftarrows \mathrm{R(aq)} \tag{3}$$

The standard reversible potential U^0 is given exactly in terms of Gibbs energies:

$$U^0 = \{G^0_{\mathrm{sol}}(\mathrm{Ox}) - G^0_{\mathrm{sol}}(\mathrm{R})\}/nF - \varphi/F \tag{4}$$

where $G^0_{\mathrm{sol}}(\mathrm{Ox}) - G^0_{\mathrm{sol}}(\mathrm{R})$ is the reaction Gibbs energy for eq (3) in solution at standard conditions, F is Faraday's constant, φ is the work function of the standard hydrogen electrode, and n is the number of electrons transferred.

Each reactant and product Gibbs energy used in eq (4) was calculated as the sum of components as follows:

$$G = E + \Omega_{\mathrm{ss,nonel}} + \Omega_{\mathrm{is,nonel}} - TS_{\mathrm{e}} - TS_{\mathrm{i}} + H_{\mathrm{vib}} - TS_{\mathrm{vib}} \tag{5}$$

In eq (5) G is the total Gibbs free energy for the solute in bulk solution, E is the internal energy, $\Omega_{\mathrm{ss,nonel}}$ and $\Omega_{\mathrm{is,nonel}}$ are the respective free energies from non-electrostatic solute-solvent and ion-solute interactions, T is temperature, and S_{e} and S_{i} are entropies of the electrons and ions and $H_{\mathrm{vib}} - TS_{\mathrm{vib}}$ are the atom vibrational contributions to the free energy. The $H_{\mathrm{vib}} - TS_{\mathrm{vib}}$ contributions

were calculated using the Gaussian 09 program because it has the steps automated.[21] The method is fully described in ref 20.

Calculations of internal energies were done using the RPBE functional because of its accuracy for metal-oxygen bond strengths.[22] The entropies of translation and rotation of the solvated species were approximated by using the calculated values for the gas phase molecules as obtained using the Gaussian program. In case of water, this approximation overestimates the total entropy by about (0.015kcal/mol K) because the translational and rotational motions are actually restricted in solution by strong hydrogen bonds.[23] The exact error in case of methanol and O-H containing species is unknown. It is also unknown if there is entropy error in case of intermediates that do not form hydrogen bonds. However, errors are cancelled in most the elementary steps due to the presence of hydrogen bonds in both products and reactants in the oxidation reactions. Since thermal contributions were calculated for gas phase molecules, it was necessary to add a term that corresponds to Gibbs energy of condensation or dilution to take into account the change in concentration between the 1.0 bar standard gas pressure and the 1.0 M standard solution concentration at 298.15 K. This concentration term, G_{conc}, was approximated using the equation

$$G_{conc} = k_B T \ln(C_2/C_1) \quad (6)$$

where k_B is the Boltzmann constant, T is the temperature, C_1 is the molar concentration corresponding to 1.0 bar gas pressure and equals 1/24.46 mol/L. C_2 is the molar concentration for the liquid phase and equals 55.3 mol/L for H_2O(l) or 1.0 mol/L for any other species. The activity coefficient was assumed to be unity in these calculations. G_{conc} is added as an additional contribution to G in eq (5).

The reversible potentials for the surface reactions, U_{surf}^{rev}, are given to good approximation by[17]

$$U_{surf}^{rev} = U^0 + [\Delta_{ads}G(P) - \Delta_{ads}G(R)]/nF \quad (7)$$

In this equation the $\Delta_{ads}G$ are adsorption Gibbs energies at the potential of zero charge, and for the oxidized intermediates (reactants in eq 3) they are $\Delta_{ads}G(Ox)$, given by

$$\Delta_{ads}G(Ox) = G(Ox(ads)) - G(surf) - G(Ox) \quad (8)$$

Similarly, for the reduced intermediates, R (adsorbed component of the products)

$$\Delta_{ads}G(R) = G(R(ads)) - G(Surf) - G(R) \quad (9)$$

In the LGER approximation the adsorption Gibbs energies are approximated using the formula

$$U_{surf}^{rev} \approx U^0 + [\Delta_{ads}E(Ox) - \Delta_{ads}E(R)]/nF \quad (10)$$

where the adsorption internal energies are calculated at the potential of zero charge. Equation (10) is the formula used in this paper.

In implementing eq (10), the internal energies were calculated using the two-dimensional band theory option on the Interface code. The first contribution to the Gibbs energy in eq (5), namely *E*, was calculated for each reactant or product intermediate first isolated in vacuum and then adsorbed at the surface-vacuum interface, omitting zero-point energies. The LGER procedure predicts reversible potentials with errors less than 0.2 V, with occasional outliers of 0.3 V; experience shows that results using *G* values from eq (5) have similar error ranges.[17]

Adsorbed states were modeled for 1/6 monolayer coverage as shown for methanol as an example in Figure 2 with the translational cell outlined. An 18 atom, 3×2 unit cell with 2-

dimentional periodic boundary condition was used to generate a three-layer thick slab model of the bulk surface. The 6 atoms in the bottom layer were fixed in the calculated bulk structure with lattice constant 4.03 Å.[20] A 3×6×1 grid was used for the Monkhorst-Pack sampling[24] in the Brillouin-zone.

The reversible potentials may also be calculated using the procedure of calculating Gibbs energies of reactants and products as functions of electrode potential and identifying the equilibrium condition as the crossing point, which is the predicted reversible potential.[17,20] This procedure is perhaps 0.1 V or 0.2 V more accurate than using the LGER approach of Eq. (10). It is advantageous to use the LGER approach in the present study because of the large number of reactions. There are other approaches to estimating reversible potentials for electrode surface reactions, many discussed in a recent somewhat personalized review.[25] One is an ad hoc approach wherein adsorption energies are assumed to depend on electric fields of strengths estimated for different the applied potentials. Several parameters must be set and the potential of zero charge is used for the calculations of energies. The Interface program uses the full Hamiltonian and electric fields may be calculated using the resulting self-consistently converged electron density distribution functions. With the predictions of electrode potential-dependent chemical properties already in hand from Interface calculations, it is unnecessary to derive and discuss the electric fields. However, in the present work we use the simpler LGER model with adsorption internal energies calculated at the potential of zero charge and electrolyte omitted so any calculated electric fields will be only for the vacuum interface.

C. Results for methanol oxidation

a. Reversible potentials for the solution-phase reactions

The first two columns of numbers in Table 1 give the calculated standard reaction Gibbs energies for the solution reactions, $\Delta G^0_{sol} = G^0_{sol}(Ox) - G^0_{sol}(R)$ used in eq (4), and the resulting calculated standard reversible potentials. It is seen that there is a wide, 5.5 eV range, in the reversible potentials. It is the job of a good catalyst to focus these on 0.032 V, which is the experimental value for the 6-electron oxidation. Since the reactions are written as oxidation, the reversible potentials have the same signs as ΔG^0_{sol}. Some are very positive, such as for the initial oxidation of the methyl group CH bond in methanol to form hydroxymethyl, $HOCH_2$,

$$HOCH_3(aq) \rightarrow HOCH_2(aq) + H^+(aq) + e^- \qquad 1.388\ V \qquad (11)$$

and its subsequent oxidation to hydroxymethylene, HOCH,

$$HOCH_2(aq) \rightarrow HOCH(aq) + H^+(aq) + e^- \qquad 1.057\ V \qquad (12)$$

and hydroxymethylene oxidation to hydroxymethylidyne, HOC,

$$HOCH(aq) \rightarrow HOC(aq) + H^+(aq) + e^- \qquad 0.662\ V \qquad (13)$$

The trend to lower reversible potentials is a result of the remaining C-H bond strengths increasing by about 0.4 eV as each H is lost. HOC oxidation to CO, however, has a very negative potential because H bonds weakly to the O end of CO and, furthermore, CO is stabilized by has a strong triple bond,

$$HOC(aq) \rightarrow CO(aq) + H^+(aq) + e^- \qquad -2.955\ V \qquad (14)$$

Oxidation of the methanol hydroxyl group OH bond to form methoxy, OCH_3, has a high potential,

$$HOCH_3(aq) \rightarrow OCH_3(aq) + H^+(aq) + e^- \qquad 1.862\ V \qquad (15)$$

but its oxidation to formaldehyde, OCH_2 has a negative potential because formaldehyde is stabilized by the C-O double bond,

$$OCH_3(aq) \rightarrow OCH_2(aq) + H^+(aq) + e^- \qquad -1.416\ V \qquad (16)$$

There is no CO bond stabilization upon formaldehyde oxidation to formyl, OCH; in fact the CO bond is destabilized, resulting in a positive oxidation potential,

$$OCH_2(aq) \rightarrow OCH(aq) + H^+(aq) + e^- \qquad 1.157\ V \qquad (17)$$

Formyl oxidation to CO has a negative potential because of forming the triple bond,

$$OCH(aq) \rightarrow CO(aq) + H^+(aq) + e^- \qquad -1.449\ V \qquad (18)$$

From the potentials for eqs (14) and (18), it is seen that the dissociation Gibbs energy for the H-OC bond is 1.506 eV less than for the OC-H bond. It is similar considerations of bond strengths that explain predictions of the LGER method for adsorbed reactants and/or products.

Three reaction Gibbs energies for non-electron transfer steps are also shown in Table 1, adding OH to CO for CO oxidation, adding OH to OCH for HOOCH formation and removal of the acidic H. Other oxidation reactions included in Table 1 are for OH formation from H_2O oxidation, and reaction possibilities for formic acid oxidation. All will be used later for analysis of the electrocatalysis.

Finally, the calculated standard reversible potential for the six-electron oxidation of eq (1) is -0.095 V. This is 0.127 V less than the 0.032 V experimental value. The agreement is not exact because theory has approximations but this error is within the range seen in previous applications of the theory.[19]

b. Comment on mechanism for H atom removal

Past work using this theory dealt with oxygen reduction, a reaction that takes place on cathodes in fuel cells at potentials near the upper end of the double layer region for platinum and platinum alloys, above about 0.6 V. As discussed above, in this potential region there is no adsorbed H and the reduction involves proton transfer from a solvated hydronium ion and concomitant electron transfer from the electrode. The upd H(ads) exists on the surfaces at potentials below around 0.4 V, having formed in acid electrolyte by hydronium ion reduction to form metal-hydrogen sigma bonds. As the electrode potential is decreased toward zero, the equilibrium concentration of upd H(ads) increases toward one monolayer, and evolution of H_2 commences. In the following we calculate reversible potentials to be negative for some intermediate steps and they will have low activation energies at positive potentials.

If H(ads) were to form by metal insertion into the CH or OH bonds in the potential region near 0.0 V and form H_2, the reaction would be non-productive because no current would be generated. The power of the fuel cell will be reduced by this dehydrogenation reaction if it occurs. On the other hand, if surface metal atoms insert into the CH or OH bonds in the potential regions of upd H(ads) and then the H(ads) are oxidized forming $H^+(aq) + e^-$, the dehydrogenation will be productive and contribute to the anode current in this potential range. We have not calculated activation energies for the insertion reactions.

c. Reversible potentials on the Pt(111) electrocatalyst surface

Calculated adsorption internal energies used in this work in the LGER applications are listed in Table 2 and their structures are shown in Figure 3. For some of the adsorbates, the adsorption sites were chosen taking into account the tetravalence of carbon. Thus O-CH_3 bonds through the

O atom to a 1-fold atop site and HO-CH_2 bonds through C to an atop site. It is noted that when placed initially over bridge and 3-fole hollow fcc sites, $HOCH_2$ the variational calculations moved it to the most stable 1-fold site. HO-C-H bonds through the C atom to a 2-fold bridge site, O=C-H bonds through C to an atop site, HO-C bonds through the C atom to a fcc 3-fold bridging site 0.100 eV more strongly than to the hcp 3-fold site, HO-C=O bonds through C to an atop site. All of these molecules adsorb strongly. Formaldehyde, O=CH_2 adsorbs weakly by back-donation to π^* bonding and takes a di-σ bridging structure. Of the remaining molecules, CO adsorbs strongly in the 2-fold site though the 1-fold site is known experimentally to be the adsorption site for low coverage. This is a well-known failure of standard density functional theories and has been shown to be corrected when all electron scalar relativistic calculations are performed.[26] We use the 2-fold site adsorption energy and note that calculated adsorption energies are slightly weaker at the 3-fold fcc, hcp and 1-food sites by < 0.01 eV, 0.03 eV and 0.22 eV, respectively. OH bonds strongly and OH_2 weakly at atop sites with the OH bonds nearly parallel to the surface, as shown in Ref. 19. H-O-CH_3 bonds weakly with the O-H bond nearly parallel to the surface, like OH_2. OCO and HOOCH adsorb very weakly. The OCO adsorption energy is most stable when parallel with the O atoms bridging and is 0.01 eV less stable parallel with the C atom atop and when it bonds perpendicularly through O at an atop site it is only 0.02 eV less stable. This is as expected for van der Waals bonding and, correspondingly, the respective distances to the surface atom plane are 3.72 Å , 3.78 Å, and 4.04 Å. $OOCH^-$ is closed-shell like formic acid and adsorbs weakly. The energies in Table 2 were used to generate the reaction scheme in Figure 4. The different branches in this scheme are discussed next.

1. Steps to CO_2: CO and non-CO pathways

Looking in Table 2 at the series methanol, $HOCH_2$, HOCH, HOC, it is seen that $\Delta_{ads}E$ increases steadily as more C-H bonds are removed. This means the solution phase standard reversible potentials for the first three reactions in Table 1 will be less on the surface, and as Table 1 shows, they are -0.743 V, 0.083 V, and -0.575 V, respectively. All three of these one-electron transfer steps should have low activation energy barriers at positive potentials according to the logic of applying the general shape in Figure 1 to these reactions. Alternatively, if H is transferred onto a metal site first by Pt insertion into the HC bond of the adsorbate, the activation barrier is controlled by this addition step and is only weakly dependent on the electrode potential. These activation energies have yet to be determined.

The oxidation of methanol to OCH_3(ads) has a high reversible potential, 0.423 V, which may make its formation uncompetitive with $HOCH_2$ formation as the first oxidation step when the electrode potential is less than 0.423 V. In the literature it has been proposed that the first step in methanol oxidation under electrochemical conditions is the C-H scission because the O-H bond is held intact by hydrophilic/hydrophobic interactions and by the local electric field.[27] The calculated U_{surf}^{rev} values show that, based on reversible potentials, the CH bond should be oxidized preferentially to the OH bond, generating current when the anode potential is less than 0.4 V.

All mechanisms studied are displayed in a reaction network in Figure 4. A dual oxidation pathway has long been proposed.[2,3,28] The figure shows our findings support this. After OCH(ads) forms, the reversible potential for oxidation to CO(ads), -0.697 V, means this step is very favorable at positive electrode potentials. CO(ads) then reacts with OH(ads) in a slightly, 0.195 eV, endothermic reaction, to form HOCO(ads), which is oxidized with a low reversible potential, 0.179 V, to CO_2. This has been referred to as the "CO pathway" and the "indirect path." On the other hand some OCH(ads) can react, also in a slightly, 0.190 eV, endothermic

reaction, with HO(ads), to form formic acid, which is oxidized with two paths available, both having low reversible potentials. These would be referred to as "non-CO" pathways or "direct path" pathways. Further discussion of formic acid oxidation will be given later.

2. Formaldehyde formation

Figure 4 shows two paths to formaldehyde and both have steps with high reversible potentials, and they will restrict OCH_2 formation to high potentials. The calculated reversible potentials are 0.423 V for OCH_3(ads) formation from methanol and 0.642 V for OCH_2 formation from $HOCH_2$(ads). Formaldehyde adsorbs relatively weakly, 0.546 eV, though stronger than HOOCH, at 0.11 eV, and this should allow some OCH_2 to enter the bulk solution, especially on a congested surface, before it can become oxidized to OCH(ads).

As explained in the Abruna review, the quantity of OCH_2 that is formed during methanol oxidation is highly variable, depending on platinum catalyst conditions such as surface roughness.[3] Early work on platinum for 1.0 M methanol in 1.0 M sulfuric acid at 0.6 V yielded OCH_2 along with HOOCH, methyl formate, CH_3OOCH, and carbon dioxide.[29] Korzeniewski and coworkers measured OCH_2 formation over polycrystalline platinum in 0.10 M perchloric acid at potentials ranging from about 0.4 V to 0.8 V.[30] The reversible potentials calculated for the two paths to OCH_2, 0.432 V and 0.642 V, lie in this range. For polycrystalline surfaces platinum sites of lower coordination at steps and grain boundaries will bond OCH_3(ads) more strongly compared to (111) face sites and there will some decrease $U_{\text{surf}}^{\text{rev}}$ for OCH_3(ads) formation compared to the results in Table 1 and Figure 4. Computed adsorption internal energies from DFT slab-band Vienna ab initio simulation package (VASP) calculations in the literature for methanol, OCH_3(ads), and $HOCH_2$(ads) on Pt(111) and step sites of Pt(211) show

such changes.[31] Strengthening the OCH_3(ads) adsorption bond strength to the catalyst will not impede OCH_2 formation which will continue to have low U_{surf}^{rev}. Strengthening the bonding of $HOCH_2$(ads) to the surface would lower U_{surf}^{rev} for the other pathway to OCH_2, but, based on the adsorption energies in ref 31, the shift would be less than for OCH_3(ads) formation.

Batista et al. investigated the oxidation of 1.0 M methanol on Pt(111) in 0.1 M $HClO_4$ and 0.5 M H_2SO_4 at 0.6 V.[32] High performance liquid chromatography (HPLC) was used to analyze the products. From the formic acid, formaldehyde, and carbon dioxide product distributions it was found that while all three formed in $HClO_4$, in sulfuric acid carbon dioxide was largely suppressed. It was proposed that adsorbed sulfate ions allowed methanol molecules to approach the restricted surface in such a way as to require its OH bond to be oxidized first, forming OCH_3(ads) which could then be oxidized to OCH_2. It may be seen in Figure 3 that the first oxidation intermediate $HOCH_2$(ads) does in fact occupy more space on the surface than OCH_3(ads). However, further work remains to establish the validity of the hypothesis.

Housmans et al. in a more recent study concluded that over Pt(111) electrodes in 0.5 M sulfuric acid the OCH_3 route seemed favored.[33] Their basis was the observed amount of CH_3OOCH(aq) relative to the amount of carbon dioxide in their experiments. Methyl formate forms in solution from the reaction of aqueous methanol and the partial oxidation product, HOOCH(aq). Formic acid formation was associated with the OCH_3(ads) pathway, which was thought to lead predominately to soluble intermediates. The $HOCH_2$(ads) pathway was thought to predominately lead to carbon monoxide and then to carbon dioxide. The CH_3OOCH to carbon dioxide mass ratio was 3.3 for the H_2SO_4 electrolyte and 1.5 in 0.5 M $HClO_4$, which means there actually was not a large difference between the relative amounts of products formed during

methanol oxidation in the two electrolytes, but in H_2SO_4 more HOOCH was forming than in $HClO_4$. In support, our work shows that both pathways can lead to HOOCH via OCH(ads).

A monitoring of the electrochemical oxidation of 0.5 M methanol on a Pt thin film electrode in 0.1 M $HClO_4$ was done by recording in situ surface enhanced infra-red absorption (SEIRA) spectra during measurement of a cyclic voltammogram.[32] It was seen that as the absorption band intensity of CO(ads) decreased with increasing potential, another band attributed to formate, OOCH(ads), started to rise at 0.5 V. This band was accompanied by an increase in the faradic current. Based on this observation, the authors concluded that at least some of the CO_2 was produced by the oxidation of OOCH(ads) and not CO.[32] In possible support, Wieckowski and Neurock et al. used a combination of chronoamperometry and fast scan cyclic voltammetry and found a secondary pathway became active at potentials > 0.35 V, with increasing contribution at higher potentials.[31] Also, early work using in situ Fourier transform infrared spectroscopy (FTIR) and polycrystalline Pt electrode, identified hydrogenated species such as COH(ads) and H_xCOH(ads) along with CO(ads) when potential was held at 0.35 V.[34]

3. Comments on the experimental observations of adsorbed intermediates

The experimental search for the intermediates OCH(ads), HOC(ads) and others on platinum single crystalline surfaces has been inconclusive. For example, Xia et al. obtained in situ FTIR spectra indicating the presence of HOC(ads) and other $HOCH_x$(ads) species during methanol electrooxidation.[34] However, Chen et al. pointed out that there seemed to be a problem of lack of reproducibility of such results among different groups and in their surface-enhanced infrared adsorption spectroscopic (SEIRAS) study using Pt film electrodes they found only two adsorbed

intermediates, CO(ads) and OOCH(ads), the latter which they presumed to be in the form of the anion.[35] The formyloxy, OOCH(ads) radical by itself bonds strongly, 2.112 eV in our calculation, and the formate anion, $OOCH^-$(ads), weakly, 0.345 eV. Moreover, the calculated reversible potential for oxidizing $OOCH^-$(aq) is 0.038 V, which means that in the potential range of 0.6 V to 1.0 V, where the adsorbed species is observed by SEIRAS, it is in the form of adsorbed OOCH. According to the calculated reversible potential for its oxidation to CO_2, -0.500 V, it might be expected to be unstable in this high range of potentials. We cannot account for this disagreement with a high confidence level, but suggest that hydrogen bonding of coadsorbed water molecules would stabilize OOCH(ads)and thereby shift the reversible potential for their oxidation to CO_2 in the positive direction. The OOCH(ads) has a structure particularly well-suited for this because the two O atoms are on the surface, as would be water molecules which adsorb with their planes nearly parallel to the surface plane. There is also the possibility of unusually large activation energy at U_{surf}^{rev} in this case because during the oxidation two O bonds to the surface must be broken, along with the CH bond. Support for this suggestion is found in the results of calculations of Neurock et al. Using a model for the electrochemical interface, activation energies of 1.0 eV and greater were calculated.[36] Experimental studies that will be discussed in the next section have led to a mechanism for OOCH(ads) radical oxidation where the electron transfer step is not rate limiting for its oxidation.

4. Formic acid formation

As shown in Figure 4, all the $HOCH_x$(ads) intermediates have low predicted oxidation potentials and should be intermediates for forming CO(ads) and OCH(ads) at the positive potentials of interest. If OH(ads) is present it can nab OCH(ads) to form formic acid which, if it

doesn't desorb, forms OOCH(ads) or hydroxyformyl, HOCO(ads) radicals which can be oxidized to CO_2. One or both of these routes corresponds to a "direct" path.

The LGER prediction for the reversible potential for forming OH(ads) is 0.494 V, which is at the low end of the reported range, 0.5-0.7 V.[4-8] On defect sites and edge sites of polycrystalline surfaces the reversible potential for OH(ads) formation will be even less because OH bonds more strongly to such sites and to have the equilibrium condition the electron is destabilized by an amount equal to the strengthening of the OH adsorption bond. The OH(ads) can react with OCH(ads) to form HOOCH in a reaction that is 0.190 eV endothermic. Or OH(ads) can react with CO(ads) to form HOCO(ads) in a reaction that is 0.195 eV endothermic. Both of these molecules can be oxidized to CO_2.

The HOOCH forms a weak 0.111 eV bond to the surface and when adsorbed it dissociates to $OCHO^-$(ads) + H^+(aq), gaining small 0.003 eV stabilization. The $OOCH^-$(ads) are oxidized with a low 0.038 V reversible potential to become OOCH(ads), which can be oxidized to CO_2. Oxidation of the CH bond in formic acid has a very favorable reversible potential of -0.692 V and this is followed by oxidation of the OH bond at slightly positive potential, U_{surf}^{rev} = 0.227 V.

5. Experimental background for formic acid oxidation

There continues to be activity to understand the electro-oxidation of formic acid over platinum electrodes and progress to this goal has advanced substantially during the last decade.[36-45] The interest in this topic goes back many decades and the reader is referred to the references for discussions of earlier work and for entries into the older literature. The topic has also attracted computational work using density functional theory.[36, 40, 41, 44] References 36-44 all

include discussions of multiple pathways for the electrooxidation of HOOCH to CO_2. All deal with mechanisms in acid electrolyte except for the study in ref 43 using base.

In 2006 the Osawa group showed using SEIRAS that CO is produced by the "dehydration" of HOOCH on polycrystalline platinum in acid electrolyte.[37] This happened at potentials close to 0.0 V (RHE), and removing CO(ads) required going to higher potentials where OH(ads) could form and oxidize it. Adsorbed "formate," which we showed above is OOCH(ads), was seen at ~0.6 V and above, but its formation seemed to be blocked by CO(ads) at lower potentials, and with increasing potential it was gone by 1.2 V. Oxidation through the indirect path, through CO(ads), was found, based on isotope substitutions, to proceed at negligibly slow rate. This left the direct path, taken by earlier workers to be the oxidation of adsorbed "formate," as the one followed.

At the same time as the Osawa work, extended insight was being gained by Chen, Behm, and coworkers.[38,39] They found from infrared and kinetic isotope measurements that there is a rapid equilibrium between adsorbed "formate" (OOCH) and HOOCH in solution. They deduced that CO(ads), formed from adsorbed "formate" oxidation, contributed little to the oxidation current for HOOCH, and also that, up to 0.75 V, little oxidation current could be ascribed to the adsorbed "formate" direct pathway. To account for the observed oxidation currents, they proposed the existence of a third unidentified intermediate and its associated pathway. For the indirect CO(ads) pathway, they measured a kinetic isotope effect, $k_{CH}/k_{CD} = 1.9$ and for the observed dominant direct pathway they measured $k_{CH}/k_{CD} \sim 3$, which they associated with a lower activation energy.

Cuesta and coworkers subsequently deduced from an ATR-SEIRAS study that at potentials below about 0.45 V HOOCH was dehydrated to CO(ads) + H_2O and with no net current flow for this process.[42] This is a step in the indirect path to oxidation. For the direct path they proposed a rate-limiting step where two neighboring OOCH(ads) combined to form $2CO_2 + H_2$. The H_2 is then oxidized to $2H^+$(aq). The proposed rate-limiting step does not involve electron transfer.

Very recently Chen et al. made a series of electrochemical measurements, the results of which fit a kinetic model where CH bond activation was the rate-limiting step for the dominant direct pathway and for the first oxidation step HOOC(ads) formed.[45]

The findings in the above studies indicate that more work is needed before the experimental picture can be completely clear.

Abruna et al. studied $OOCH^-$ oxidation over polycrystalline platinum in strong base.[43] They found activity to be significantly less than for HCOOH and we attribute that to the possibility of adsorbed OOCH(ads) participating as an intermediate being excluded.

6. **Results for formic acid oxidation**

The focal point for our theoretical explanation for the observations discussed in the recent papers is the reaction scheme in figure 4. It is seen that three paths for HOOCH oxidation to CO_2 were examined.

i. Results for dehydration[CO(ads)] path to formic acid oxidation

Cuesta and coworkers noted that below 0.45 V in acid electrolyte CO formed with no net current flow.[42] Looking at figure 4, it is seen that HOOCH can decompose to OCH(ads) and OH(ads) in a 0.190 eV exothermic reaction. On the platinum surface there will have be

structural distortions in HOOCH(ads) to bring the CO bond undergoing scission into contact with platinum atoms in the surface. Such contact will be needed to activate the scission. Therefore for this step the activation energy has an undetermined value at present and awaits future calculations. Once OCH(ads) forms, it should be oxidized to CO(ads) even at the low observed potential approaching 0.0 V because its calculated reversible potential is -0.697 V, which is very negative. Concurrently, at potentials < 0.45 V, the OH(ads) will be reduced to H_2O. The overall combination of the one-electron oxidation of OCH(ads) and the one electron reduction of HO(ads) results in no net current flow, as discussed and observed by Questa and coworkers. Coverage of CO(ads) builds at low potentials and blocks reaction by the direct path(s), as at potentials < 0.45 V. At higher potentials OH(ads) is stable and it will combine with CO(ads) in a mildly (0.195 V) endothermic reaction to form HOCO(ads), for which the calculated oxidation reversible potential is low, 0.227 V; it will be oxidized to CO_2.

ii. Results for adsorbed formyloxy radical path to formic acid oxidation

Figure 4 shows two apparently easy essentially reversible paths to OOCH(ads) formation at low potentials. This reversibility with respect to the solution phase was deduced in the deuterium labeling experiments using acid electrolyte of Chen and Behm and coworkers.[38,39] In one path the HOOCH(aq) deprotonates and the $OOCH^-$(ads) then adsorbs on the surface and oxidized at low potential, the calculated reversible potential being 0.038 V. We calculated the dissociation Gibbs energy for HOOCH(aq) dissociating to $OOCH^-$(aq) and H^+(aq), obtaining 0.231 eV. This yields an equilibrium constant of $1.4x10^{-4}$ for K_a, the acid constant for HOOCH(aq), which is close to the experimental value of $1.8x10^{-4}$. Given the small acid constant, there will be little $OOCH^-$(aq) and it might be thought that this mechanism should be

followed infrequently. However, the adsorption bond strength for $OOCH^-$(aq), 0.345 eV, will allow the surface concentration to build up, making this path viable.

The second path is the direct oxidation of HOOCH molecules near the surface to form OOCH(ads). The calculated reversible potential for this is 0.034 V. As discussed earlier, the reversible potential for oxidation of OOCH(ads) is very low, calculated to be -0.500 V, but the activation energy is high, according to theoretical work of Neurock et al.,[36] making isolated OOCH(ads) a stable surface species. However, the direct path proposed by Questa and coworkers where two neighboring OOCH(ads) combine to form $2CO_2 + H_2$ would, if correct, allow reaction of OOCH(ads) when sufficiently high surface concentrations are achieved. Our calculations show that high concentrations are likely because of the stability of OOCH(ads).

iii. Adsorbed hydroxyformyl radical [HOCO(ads)] path

The calculated reversible potential of -0.692 V for HOOC (ads) formation from HOOCH is very favorable for reactivity at low potentials. But if it is so difficult to oxidize the CH in OOCH(ads), why would it not also be difficult to oxidize it in weakly adsorbed HOOCH(ads)? Neurock and coworkers found in their theoretical model that the activation energy for this step was much smaller, changing from 0.5 eV to 0.42 eV between 0 V and 1 V. This is compared to 1.2 eV at 0 V to 1.0 eV at 1 V for oxidizing OOCH(ads). The relative magnitudes are presumably accurate enough for this qualitative discussion. This is still a fairly high activation energy compared to our past work,[16] but it is much less than the energy for homolytic CH bond scission in free molecules. At potentials where the surface is not fully blocked by CO(ads), HOOCH(aq) molecules could approach the surface with the C-H bond first. The C-H bond would either dissociate by metal atom insertion into it, generating H(ads) which would be

oxidized and a metal-C bond, or it would deprotonate into solution, forming $H^+(aq) + e^-$ and the metal-C bond. Once HOOC(ads) forms, the calculated reversible potential for its oxidation, 0.227 V, is low so that CO_2 will form in this potential range.

D. Adsorption bond strengths for intermediates on the ideal methanol oxidation electrocatalyst

If all electron transfer steps during the electrooxidation of methanol on an electrocatalyst surface had reversible potentials the same as for the overall six-electron oxidation reaction the overpotentials would be controlled purely by kinetics. Otherwise, as has been shown in this lab, there is the possibility of exergonic chemical reaction steps not including electron transfer causing an effective reversible potential for the overall reaction. Such an effective potential creates a thermodynamic minimal overpotential and became the basis for understanding the limitations of platinum-based electrocatalysts used for oxygen cathodes in fuel cells. [17,46,47]

It may be seen from the reversible potentials calculated for adsorbed intermediates formed during methanol electrooxidation on Pt(111) that there is no significant exergonic chemical reaction step. There are two endergonic ones: CO(ads) reaction with OH(ads) to form HOOC(ads), 0.195 eV, and OCH(ads) reaction with OH(ds) to form HOOCH(ads), 0.190 eV. These steps will contribute to the kinetics as activation energies. If the anode potential is set to -0.095 V, which is the calculated U^0 for the six electron oxidation, then steps with reversible potentials negative of this will be spontaneous and have as yet undetermined but probably small activation energies. Several electron transfer steps have positive reversible potentials for adsorbed intermediates. These are H-O oxidation in methanol to form $H^+(aq) + e^- + OCH_3(ads)$, 0.423 V, H-O oxidation in $HOCH_2(ads)$ to form $OCH_2(ads)$, 0.642 V, and H-O oxidation in

HOOC(ads) to form CO_2, 0.227 V. These three reactions will be very slow at -0.095 V because their equilibria lie far toward the reduced sides of the oxidation reactions. Since the reactions all involve oxidizing O-H bonds, the proton is probably transferred directly into solution and the activation energies will be higher than the values at the reversible potentials. Furthermore, the OH(ads) that participates comes from H_2O(aq) oxidation, for which the calculated reversible potential is 0.495 V and this oxidation will also be very slow at -0.095 V.

Is there a set of adsorption energies for the intermediates that will cause each electron transfer step to have its reversible at the calculated U^0 for the six-electron oxidation? The answer is yes but there are six electron transfer reactions and at least nine adsorption energies, including those for methanol, water, and CO_2. We set these three values to zero, which is semi-justified because they are all weak, but, more importantly, they will be able to add to or depart readily from the surface of an ideal electrode, which is one that doesn't suffer congestion from reactants or products. Then it is easy to determine the adsorption bond strengths of the first oxidation intermediates, and, having values for these, one proceeds throughout the mechanisms in the same way to deduce the ideal adsorption bond strengths for all the other intermediates.

Here is a sample calculation. For $HOCH_3(aq) \rightleftarrows OCH_3(ads) + H^+(aq) + e^-$ the calculated reversible potential is 0.423 V. This potential shifts to -0.095 V if the adsorption bond strength is increased from the calculated value 1.439 eV by 0.518 eV to become 1.957 eV. The 0.518 eV increase comes from destabilizing the electron by 0.423 eV + 0.095 eV. The new value and difference between it and the calculated adsorption bond strength are entered in Table 3. By propagating through the paths shown in figure 4 all ideal adsorption bond strengths were found and entered in Table 3. Adjustments were also made so that the energies of OH(ads) adding to CO(ads) and to OCH(ads) were zero. It is clear that CO(ads) poisons the platinum surface

because its ideal adsorption bond strength is 0.533 eV, 1.107 eV less than the calculated value. Another notable result is that in the ideal electrocatalyst for methanol oxidation the OH adsorption energy should increase by 0.59 eV but in the ideal electrocatalyst for O_2 reduction it should decrease by 0.46 eV.[47]

E. Looking at the reverse reaction: CO_2 electroreduction

While a continuing area of research, the carbon dioxide reduction processes, whether chemical, electrochemical, or photochemical, are energy intensive and so far remain inefficient.[48,49] The standard reversible potential for reduction to formic acid is about -0.20 V[49] and our calculated value is in good agreement at -0.288 V, but a potential that low is unachievable on platinum electrodes because the approach of CO_2 molecules to the surface will be disrupted by hydrogen evolution, which has a standard reversible potential of 0.0 V and for which platinum is an efficient electrocatalyst. Of many materials tried, copper has shown the most efficiency in reducing CO_2, but the product distribution is wide and overpotentials are around 1.0 V, meaning the electrocatalyst is not very active or selective.[49] There are three probable contributing factors to the poor activity, (i) poor electrocatalysis due to high activation energies, (ii) reversible potentials for certain steps leading to high overpotentials, (iii) interference from hydrogen evolution which decreases the rate at which CO_2 can reach the electrode.

It is clear that a Pt(111) electrode will not be an effective catalyst for CO_2 reduction. There will be a small shift of (1/6)(0.2 V) to an effective reversible potential 0.03 V negative of the standard reversible potential for the six-electron reduction to methanol. One significant problem lies in some of the reduction steps having reversible potentials far negative of the calculated U^0.

This means that for reduction the activation barriers can be expected to be high for these steps except at negative potentials. Paths requiring OH(ads) will suffer because of the positive potential required for oxidizing H_2O. Another significant problem is hydrogen evolution, for which platinum is an excellent electrocatalyst, will block CO_2 reaching the electrode surface. If the two-electron reduction to formic acid is allowed over a catalyst but the six-electron reduction is blocked, CO(ads) would be the blocking molecule, forming from HOOC(ads) dissociation according to the scheme in Figure 4. What is needed for effective CO_2 electroreduction is a catalyst that retards H_2 evolution and that also brings the reversible potentials for the electron transfer steps to about 0 V. A catalyst with a small with slow H_2 evolution and the adsorption energies of the ideal methanol oxidation catalyst will do this.

Recent research on CO_2 electroreduction over copper has begun to focus on mechanisms for forming the many observed products: carbon monoxide, formic acid, methane, and ethylene, as well as hydrogen from reduction of water.[49-51] Methanol is not observed and this has been ascribed to the preference for CO(ads), formed after the first reduction step of CO_2 to HOOC(ads), which dissociates to OH(ads) and CO(ads), favoring reduction to HOC(ads) over OCH(ads).[51] It was proposed that HOC(ads) is reduced to C(ads) + H_2O(l). The C(ads) is then reduced to CH_4 in four steps. The methanol forming path was proposed to begin with CO(ads) reduction to OCH(ads) but this was deemed uncompetitive due to a higher calculated activation energy.

What are the conditions for eliminating H_2 evolution when reducing CO_2? At 0.0 V H_2 is evolved because the Gibbs adsorption energy of H is equal to about half the H_2 bond strength, which is 4.4781 eV.[52] An ideal CO_2 reduction electrocatalyst will need to adsorb H atoms more weakly. Platinum is excellent at evolving H_2 with negligible overpotential, and on copper, on

which H bonds around 0.3 eV more weakly,[53] so no underpotential H(ads) deposition takes place. On copper the measured onset potential closed to 0.0 V and strongly kinetically limited, but high current densities commence at approximately -0.2 to -0.4 V (SHE), depending on the temperature.[50] Such an overpotential is favorable for methanol oxidation anodes. The negative onset potential for H_2 evolution over copper electrodes is easily understood. Since for the reaction

$$H^+(aq) + e^-(V) + Cu \rightleftarrows H(ads) \quad (19)$$

the H adsorption bond strength is about 0.3 eV weaker than for forming H(ads) on platinum, to maintain the equilibrium on Cu of eq (19), the electron must be destabilized about 0.3 eV and this is done by decreasing the electrode potential by about 0.3 V. Once H(ads) forms it is available for H_2 evolution as an undesired side reaction and for desired reduction reactions.

F. Concluding comments

It is of interest to compare what we learned in recent studies of O_2 reduction on platinum and platinum alloy electrocatalysts used in fuel cells[47] with the above findings for the platinum anode. At the cathode, platinum based catalysts were found to have an effective reversible potential corresponding to overpotential of about 0.4 V and the observed ~0.8 V reduction reaction onset potential. This was caused by Gibbs energy loss of about 1.2 eV as heat and entropy during a non-electron transfer step, OOH(ads) dissociation to form O(ads) + OH(ads). To overcome this limitation, catalysts are needed that can adsorb O and OH more weakly than platinum and its alloys and adsorb OOH more strongly. The observed scaling relationship between the adsorption energies of these intermediates on metals means other types of materials need to be tested.

For the methanol-CO_2 reaction on platinum we found the CO(ads) + OH(ads) combination to be 0.195 eV endothermic during oxidation and so it will not cause an effective reversible potential. However for reduction it will cause a small effective reversible potential that is only -(0.195/6)V = -0.032 V less than -0.095 V. The route through formic acid also sees a small 0.045 V negative shift during reduction due to the OH(ads) + OCH(ads) combination being 0.272 eV endothermic. The problem for oxidizing methanol over platinum is mainly the high potential needed to generate OH(ads) to oxidize the four-electron oxidation intermediate CO(ads), which forms so readily at potentials above 0.0 V. The formic acid route also requires OH(ads) and so occurs at corresponding high potential.

The ideal adsorption energies in Table 3 can be used for several pathways. For the methanol oxidation pathway $HOCH_3 \rightarrow HOCH_2(ads) \rightarrow HOCH(ads) \rightarrow OCH(ads) \rightarrow CO(ads) \rightarrow HOOC(ads) \rightarrow CO_2$ a site that bonds $HOCH_2$(ads), HOCH(ads), OCH(ads), and HOOC(ads) about 0.5 eV more weakly would be ideal, but CO(ads) would have to bond 1.1 eV more weakly and it is unlikely a single type of atom would affect these changes. However, atom sites that weaken all of these adsorption energies would offer improvement over platinum. There would have to be adjacent sites that activate water oxidation to OH(ads) to finish the oxidation and these require OH(ads) to bond 0.590 eV more strongly. This will require a different type of atom, that is, the development of a dual component catalyst. If a metal less electropositive than platinum provides the needed weakening of the intermediates containing C, a more electropositive metal alloyed with it could provide the needed increase in the OH adsorption bond strength at adjacent sites. These new potential catalysts will also have to be evaluated for poisoning by upd hydrogen atoms and disruption by hydrogen evolution. For fuel oxidation pathways on either an improved catalyst or an ideal catalyst, the potential range of upd hydrogen

formation will need to be suppressed at the operating potential. For CO_2 reduction pathways, the hydrogen evolution potential will need to be as close to operating potential as possible. We hope that our findings will spur the search and discovery of new improved electrocatalysts for fuel electro-oxidation and CO_2 electro-reduction.

Acknowledgments

Dr. Haleema Asiri gratefully acknowledges generous graduate fellowship support from the Saudi Arabian Cultural Mission, and she expresses her appreciation to Dr. Ryosuke Jinnouchi for assistance with setting up the Interface code on the Case cluster. Ms. Meng Zhao generously helped with some of the calculations. Preparation of the manuscript was aided by support from the National Science Foundation under Grant No. CHE-0809209.

References

1. Wang, H.; Loffler, T.; Baltruschat, H. *J. Appl. Electrochem.* **2001**, *31*, 759-65.

2. Iwasita, T. *Electrochim. Acta* **2002**, *47*, 3663-3674.

3. Cohen, J. L.; Volpe, D. J.; Abruna, H. D. *Phys. Chem. Chem. Phys.* **2007**, *9*, 49-77.

4. Markovic, N. M.; Ross, P. N. *CATTECH* **2000**, *4*, 110-126.

5. Iwasita, T.; Xia, X. H. *J. Electroanal. Chem.* **1996**, *411*, 95-102.

6. Markovic, N. M.; Schmidt, T. J.; Grgur, B. N.; Gasteiger, H. A.; Behm, R. J.; Ross, P. N. *J. Phys. Chem. B* **1999**, *103*, 8568-8577.

7. Climent, V.; R. Gomez,R.; Orts, J. M.; Feliu, J. M. *J. Phys. Chem. B* **2006**,*110*, 11344-11351.

8. Wakisaka, M.; Suzuki, H.; Mitsui, S.; Uchida, H.; Watanabe, M. *Langmuir*, **2009**, *25*, 1897-1900.

9. Gomez, R.; Orts, J. M.; Alverez-Ruiz, B.; Feliu, J. M. *J. Phys. Chem. B* **2004**, 108, 228-238.

10. Strmcnik, D.; Tripkovic, D.; van der Vliet, D.; Stamenkovic, V.; Markovic, N. M. *Electrochem. Comm.* **2008**, 10, 1602-1605.

11. Asiri, H.; Anderson, A. B. *J. Phys. Chem. C* **2013**, *117*, 17509-17513.

12. Jusys, Z.; Behm, R. J. *J. Phys. Chem. B* **2001**, *105*, 10874-10883.

13. Anderson, A. B.; Albu, T. V. *J. Am. Chem. Soc.* **1999**, *121*, 11855-11863.

14. Gurney, R. W. *Proc. Roy. Soc*., **1931**, *134A*, 137-154.

15. Anderson, A. B.; Neshev, N. M.; Sidik, R. A.; Shiller, P. *Electrochim. Acta* **2002**, *47*, 2999-3008.

16. Zhang, T.; Anderson, A. B. *J. Phys. Chem. C* **2009**, *113*, 3197-3202.

17. Anderson, A. B. *Phys. Chem. Chem. Phys.* **2012**, *14*, 1330–1338.

18. Stanbury, D. M. Reduction Potentials Involving Inorganic Free Radicals in Aqueous Solution, *Advances in Inorganic Chemistry* **1989**, *33*, 69-138.

19. Jinnouchi, R.; Anderson, A. B. *J. Phys. Chem. C* **2008**, *112*, 8747–8750.

20. Jinnouchi, R.; Anderson, A. B. *Phys. Rev. B* **2008**, *77*, 245417-1-18.

21. Gaussian 09, Revision A.1, Frisch, M. J. et al. Gaussian, Inc., Wallingford CT, **2009**.

22. Hammer, M.; Hansen, L. B.; Nørskov, J. K. *Phys. Rev. B* **1999**, *59*, 7413–7421.

23. Siebert, X.; Amzel, L. M. *PROTEINS: Structure, Function, and Bioinformatics* **2004**, *54*, 104–115.

24. Monkhorst, H. J.; Pack, J. D. *Phys. Rev. B* **1976**, *13*, 5188–5192.

25. Studies using different models are found throughout the literature. Some of them have been discussed briefly and in a somewhat personalized manner in K-Y Yeh, and M. Janik, *Computational Catalysis* **2014**, Chapter 3, 116-156.

26. Orita, H.; Itoh, N.; Inada, Y. *Chem. Phys. Lett.* **2004**, *384*, 271-276.

27. Franaszczuk, K.; Herrero, E.; Zelenay, P.; Wieckowski, A.; Wang, J.; Masel, R. I. *J. Phys. Chem.* **1992**, *96*,2509-2516.

28. Barbaro, P.; Bianchin, C. *Catalysis for Sustainable Energy Production*: WILEY-VCH Verlag GmbH & Co. KGaA, Weinheim, Germany, **2009**.

29. Ota, K-I; Hakagawa, Y.; Takahashi, M. *J. Electroanal. Chem*. **1984**, *179*, 179-186.

30. Korzeniewski, C.; Childers, C. L. *J. Phys. Chem. B* **1998**, *102,* 489-492.

31. Cao, D.; Lu, G.-Q.; Wieckowski, A.; Wasileski, S. A.; Neurock, M. *J. Phys. Chem. B* **2005**, *109,* 11622-11633.

32. Batista, E. A.; Malpass, G. R. P.; Motheo, A. J.; Iwasita, T. *Electrochem. Commun.* **2003**, *5*, 843-846.

33. Housmans, T. H. M.; Wonders, A. H.; Koper, M. T. M. *J. Phys. Chem. B* **2006**, *110*, 10021-10031.

34. Xia, X. H.; Iwasita, T.; Ge, F.; Vielstich, W. *Electrochim. Acta* **1996**, *41,* 711-718.

35. Chen, Y. X.; Miki, A.; Ye, S.; Sakai, H.; Osawa, M. *J. Am. Chem. Soc.* **2003**, *125*, 3680-3681

36. Neurock, M.; Janik, M.; Wieckowski, A. *Faraday Disc.* **2008**, *140*, 363-378.

37. Samjeske, G; Miki, S.; Ye, S.; Osawa, M. *J. Phys. Chem. B* **2006**, *110*, 16559-16566.

38. Chen, Y.-X.; Heinen, M.; Jusys, Z.; Behm, R. J. *Langmuir* **2006**, *22*, 10399-10408.

39. Chen, Y.-X.; Heinen, M.; Jusys, Z.; Behm, R. J. *ChemPhysChem* **2007**, *8*,380-385.

40. Wang, H.-F.; Liu, Z.-P. *J. Phys. Chem. C.* **2009**, *113*, 17502-17508.

41. Gao, W.; Keith, J. A.; Anton, J.; Jacob, T. *Dalton Trans.* **2010**, *39*, 8450-8456.

42. Cuesta, A.; Cabello, G.; Osawa, M.; Gutierrez, C. *ACS Catal.* **2012**, *2*, 728-738.

43. John, J.; Wang, H.; Ris, E. D.; Abruna, H. D. *J. Phys. Chem. C* **2012**, *116*, 5810-5820.

44. Zhong, W.; Wang, R.; Zhang, D.; Liu, C. *J. Phys. Chem. C* **2012**, *116*, 24143-24150.

45. Xu, J.; Yuan, D.; Yang, F.; Mei, D.; Zhang, Z.; Chen, Y.-X. *Phys. Chem. Chem. Phys*. **2013**, *15*, 4367-4376.

46. Tian, F.; Anderson, A. B. *J. Phys. Chem. C* **2011**, *115*, 4076-4088.

47. Anderson, A. B.; Jinnouchi, R.; Uddin, J. *J. Phys. Chem. C* **2013**, *117*, 41-48.

48. Halman, M. M.; Steinberg, M. *Greenhouse Gas Carbon Dioxide Mitigation Science and Technology* Lewis Publishers, CRC Press LLC, Boca Raton, Florida, USA, **1999**.

49. Hori; Y. *Electrochemical CO_2 Reduction on Metal Electrodes*. Modern Aspects of Electrochemistry **2008**, *42*, 89-189.

50. Sharifi-Asl, S., Macdonale, D. D. J. Electrochem. Soc. **2013**, *160*, H382-H391.

51. Nie, X.; Esopi, M. R., Janik, M. J.; Asthagiri, A. Angew. Chem. Int. Ed. **2013**, 52, 2459-2462.

52. Huber, K. P.; Herzberg, G. *Molecular Spectra and Molecular Structure IV. Constants of Diatomic Molecules* Van Nostrand Reinhold Company, New York **1979**, p. 240.

53. Greeley, J.; Mavrikakis, M. *J. Phys. Chem. B* **2005**, *109*, 3460-3471.

Table 1. ΔG^0_{sol} (eV) is the calculated reaction Gibbs energy for the reactions in solution and U^0 (V) is the predicted standard reversible potential. ΔG_{surf} (eV) is the calculated reaction Gibbs energy for the reacting species when adsorbed on Pt(111) and U^{rev}_{surf} (V) is the predicted reversible potential for the reactions of adsorbed intermediates; exceptions are CH_3OH, CO_2, and H_2O, which are in the aqueous reference state. Also shown are ΔG^0_{sol} (eV) and ΔG_{surf} (eV) for reactions for which there is no electron transfer.

Reaction	ΔG^o_{sol}	U^o	[a]ΔG_{surf}	U^{rev}_{surf}
$HOCH_3 \rightarrow HOCH_2 + H^+(aq) + e^-$	1.388	1.388	-0.743	-0.743
$HOCH_2 \rightarrow HOCH + H^+(aq) + e^-$	1.057	1.057	0.083	0.083
$HOCH \rightarrow HOC + H^+(aq) + e^-$	0.662	0.662	-0.565	-0.565
$HOC \rightarrow CO + H^+(aq) + e^-$	-2.955	-2.955	-0.153	-0.153
$H_2O \rightarrow OH + H^+_{(aq)} + e^-$	2.445	2.445	0.494	0.494
$HO + CO \rightarrow HOOC$	-1.076		0.195	
$HOOC \rightarrow CO_2 + H^+(aq) + e^-$	-2.093	-2.093	0.178	0.178
$HOCH_3 \rightarrow OCH_3 + H^+(aq) + e^-$	1.862	1.862	0.423	0.423
$OCH_3 \rightarrow OCH_2 + H^+(aq) + e^-$	-1.416	-1.416	-0.523	-0.523
$OCH_2 \rightarrow OCH + H^+(aq) + e^-$	1.157	1.157	-0.689	-0.689
$OCH \rightarrow CO + H^+(aq) + e^-$	-1.449	-1.449	-0.697	-0.697
$HO + OCH \rightarrow HOOCH$	-4.012		0.190	
$HOOCH \rightarrow HOOC + H^+(aq) + e^-$	1.517	1.517	-0.692	-0.692
$HOCH_2 \rightarrow OCH_2 + H^+(aq) + e^-$	-0.943	-0.943	0.642	0.642
$HOCH \rightarrow OCH + H^+(aq) + e^-$	-0.843	-0.843	-0.130	-0.130
$HOOCH \rightarrow OOCH + H^+(aq) + e^-$	2.035	2.035	0.034	0.034
$OOCH \rightarrow CO_2 + H^+(aq) + e^-$	-2.612	-2.612	-0.548	-0.548
$HOOCH \rightarrow OOCH^- + H^+(aq)$	0.231		-0.005	
$OCOH^- \rightarrow OOCH + e^-$	1.805	1.805	0.038	0.038

Table 2. Most stable adsorption sites and adsorption energies, $\Delta_{ads}E$(eV), for reaction intermediates of methanol oxidation over the Pt (111) surface. The *stands for the atom which forms a bond to the surface. Structures are shown in Figure 3 , except for *OH and *OH_2, which may be seen in Ref 19.

Species	$\Delta_{ads}E$
methanol (H*OCH_3)	-0.277
hydroxylmethyl (HO*CH_2)	-2.131
hydroxymethylene (HO*CH)	-3.105
hydroxymethylidyne (HO*C)	-4.442
carbon monoxide (*CO)	-1.640
carbon dioxide (CO_2)	-0.048
methoxy (*OCH_3)	-1.439
formaldehyde (*O*CH_2)	-0.546
formyl (O*CH)	-2.392
hydroxyformyl radical (HOO*C)	-2.320
formyloxy radical (*O*OCH)	-2.112
formate anion ($OOCH^-$)	-0.345[a]
formic acid (HOOCH)	-0.111
*OH_2	-0.229
hydroxyl (*OH)	-1.951

a. $\Delta_{ads}G$ was used for this anion at the pzc.

Table 3. Adsorption bond strengths, *E*(ads), (eV) for the adsorbed intermediates formed during methanol on the ideal electrocatalyst. They are derived using calculated bulk solution reversible potentials and calculated adsorption bond strengths on Pt(111) at 1/6 ML coverage using the constraint that the reversible potential for each reaction step has the -0.095 V six-electron reversible potential. ΔE (eV) is the increase or decrease from the values compared to adsorption on Pt(111).

Molecule	*E*(ads)	ΔE
HOOC	1.998	-0.322
CO	0.533	-1.107
OCH	1.888	-0.504
HOC	3.394	-1.048
HOCH	2.635	-0.470
OOCH	2.517	0.405
HOOCH	0.386	0.275
$HOCH_2$	1.483	-0.648
OCH_2	0.636	0.090
OCH_3	1.957	0.518
OH	2.541	0.590

Figure captions.

1. Sketch of the general behavior of calculated electron-proton transfer activation energies calculated in the local reaction center model.[15.16]

2. Normal and oblique views defining the 1/6 ML coverage used in the calculations. The adsorbed methanol molecule is shown.

3. Pairs of adsorbed molecules on Pt(111) used in this work, all at 1/6 ML coverage as shown in Figure 2. (a) methanol, $HOCH_3$; (b) methoxy, OCH_3; (c) formaldehyde, OCH_2; (d) hydroxylmethyl, $HOCH_2$; (e) hydroxylmethylidene, HOCH; (f) formyl, OCH; (g) hydroxymethylidyne, HOC; (h) carbon monoxide, CO; (i) formic acid, HOOCH; (j) hydroxyformyl radical, HOOC; (k) formyloxyl radical or formate anion, $OOCH^-$, and (l) carbon dioxide, CO_2.

4. Summary of reactions considered and their calculated reversible potentials (V) and, when there was no electron transfer, reaction energies (eV). For clarity the $H^+ + e^-$ that accompany the oxidation products are not included. All species are adsorbed on Pt(111) except H^+(aq) formed by dissociation of adsorbed formic acid.

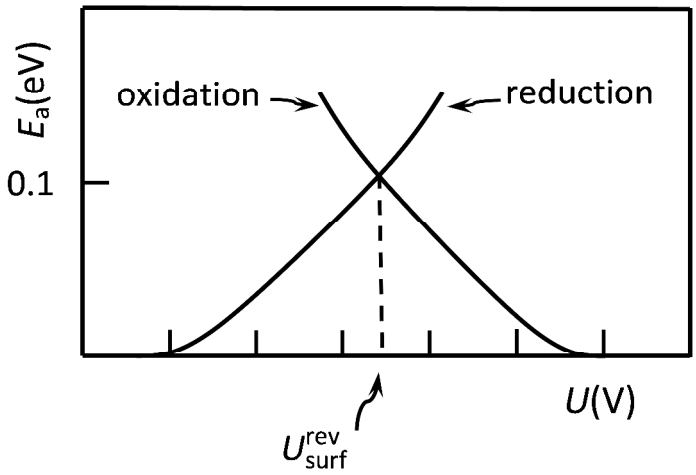

1. Sketch of the general behavior of calculated electron-proton transfer activation energies calculated in the local reaction center model.[15.16]

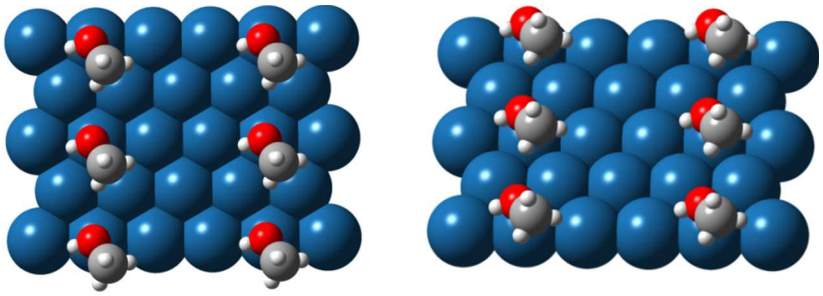

2. Normal and oblique views defining the 1/6 ML coverage used in the calculations. The adsorbed methanol molecule is shown.

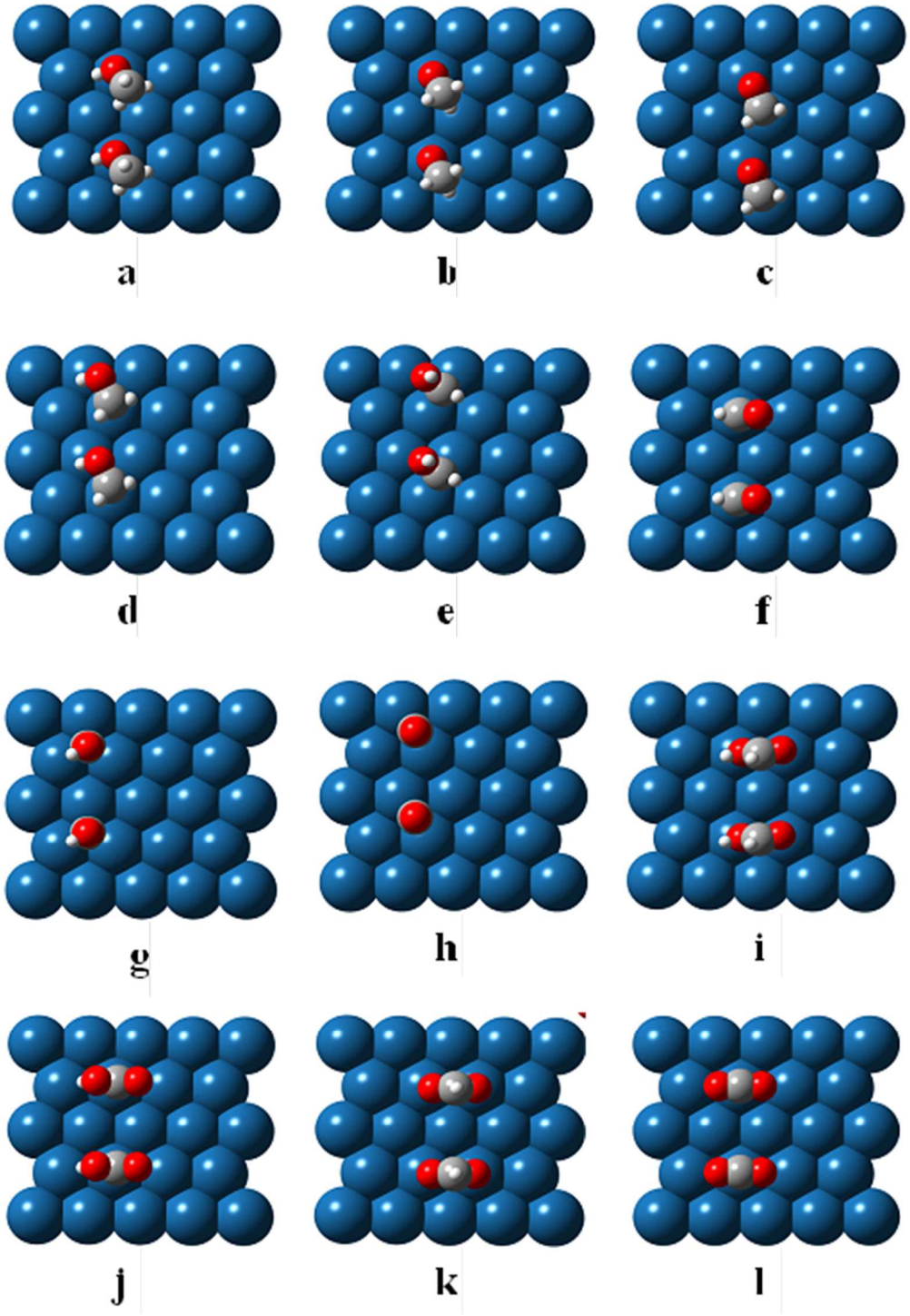

3. Pairs of adsorbed molecules on Pt(111) used in this work, all at 1/6 ML coverage as shown in Figure 2. (a) methanol, $HOCH_3$; (b) methoxy, OCH_3; (c) formaldehyde, OCH_2; (d) hydroxylmethyl, $HOCH_2$; (e) hydroxylmethylidene, HOCH; (f) formyl, OCH; (g) hydroxymethylidyne, HOC; (h) carbon monoxide, CO; (i) formic acid, HOOCH; (j) hydroxyformyl radical, HOOC; (k) formyloxyl radical or formate anion, $OOCH^-$, and (l) carbon dioxide, CO_2.

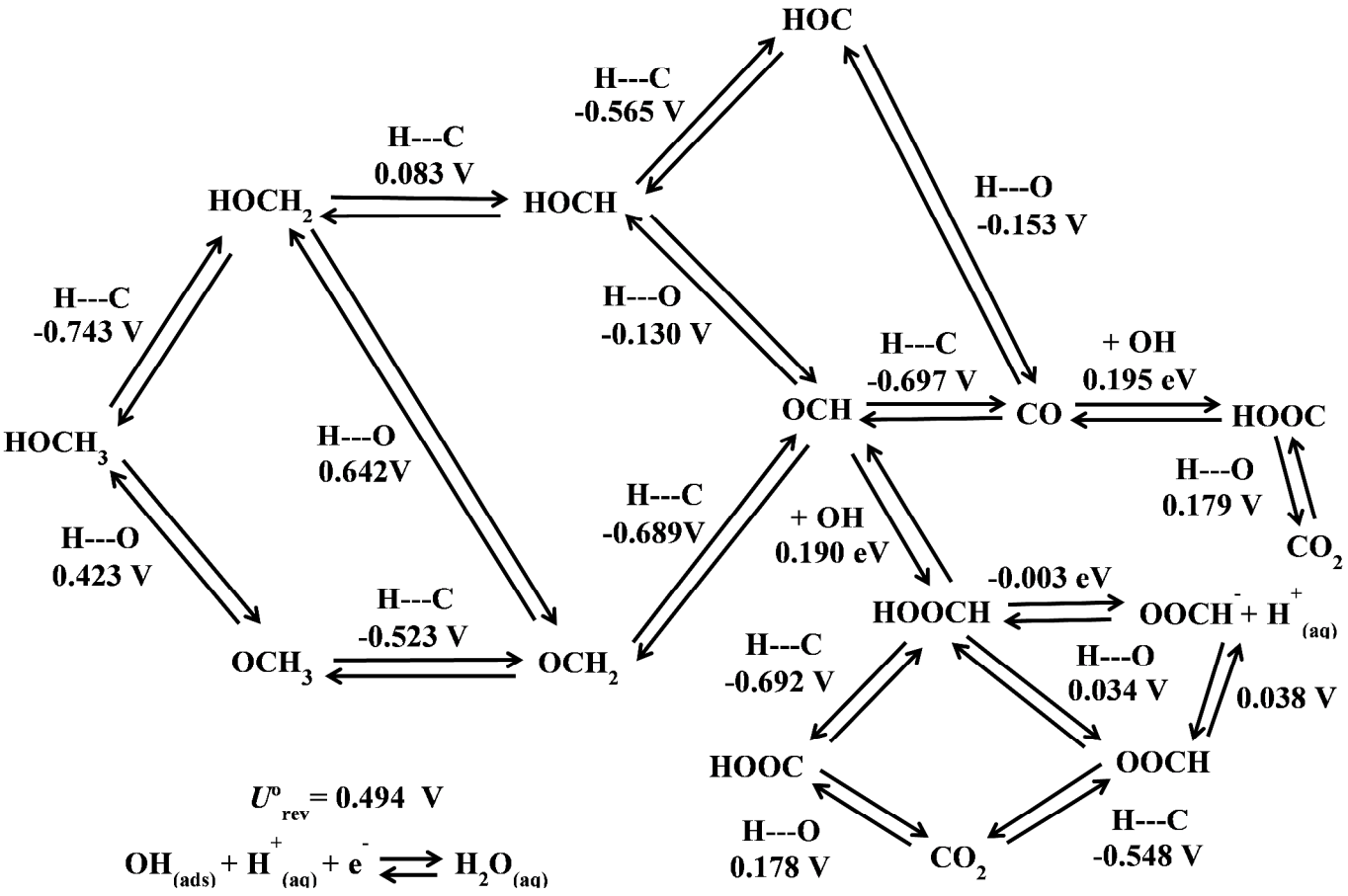

4. Summary of reactions considered and their calculated reversible potentials (V) and, when there was no electron transfer, reaction energies (eV). For clarity the $H^+ + e^-$ that accompany the oxidation products are not included. All species are adsorbed on Pt(111) except $OCHO^-$(aq) and H^+(aq) formed by dissociation of adsorbed formic acid.

Graphical abstract

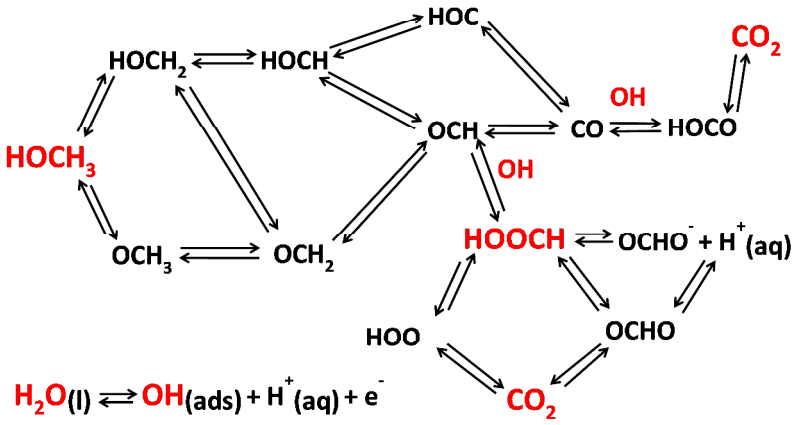

Theory has predicted reversible potentials for methanol electrooxidation on platinum and the adsorption bond strengths for the ideal catalyst.